Nanostructured RuO$_2$ on MWCNTs: Efficient catalyst for transfer hydrogenation of carbonyl compounds and aerial oxidation of alcohols

M. Gopiraman[a], S. Ganesh Babu[a,b], R. Karvembu[c,*], I. S. Kim[a,d]*

[a]*Nano Fusion Technology Research Lab, Interdisciplinary Graduate School of Science and Technology, National University Corporation, Shinshu University, Ueda, Nagano 386 8567, Japan*

[b]*SRM Research Institute, SRM University, Kattankulathur 603203, India*

[c]*Department of Chemistry, National Institute of Technology, Tiruchirappalli 620 015, India*

[d]*Interdisciplinary Cluster for Cutting Edge Research (ICCER), Division of Frontier Fibers, Institute for Fiber Engineering (IFES), Shinshu University, Ueda, Nagano 386 8567, Japan*

[a],* Corresponding author. Tel.: +81 268 21 5139; fax: +81 268 21 5482.

E-mail address: kim@shinshu–u.ac.jp (I.S. Kim).

[b],* Corresponding author. Tel.: + 91 431 2503636; fax: +91 431 2500133.

E-mail address: kar@nitt.edu (R. Karvembu).

ABSTRACT

Multiwall carbon nanotubes (MWCNTs)/ruthenium dioxide nanoparticles (RuO$_2$NPs) composite was prepared by a straightforward 'dry synthesis' method. After being well characterized, the prepared composite was used as a nanocatalyst (RuO$_2$/MWCNT) for the transfer hydrogenation of carbonyl compounds. The excellent adhesion of RuO$_2$NPs on the anchoring sites of MWCNTs was confirmed by TEM and Raman analyses. The weight percentage (7.97 wt%) and the chemical state (+4) of Ru in RuO$_2$/MWCNT was confirmed by EDS and XPS analyses, respectively. It was found that the RuO$_2$/MWCNT has a higher specific surface area of 189.3 m^2 g^{-1}. Initially the reaction conditions were optimized and then the scope of the catalytic system was extended with a wide range of carbonyl compounds. The influence of the size of RuO$_2$NPs on the transfer hydrogenation of carbonyl compounds was also studied. The RuO$_2$/MWCNT is highly chemoselective, heterogeneous in nature, reusable and highly stable. Owing to the high stability of the used catalyst (*u*-RuO$_2$/MWCNT), it was further calcinated at high temperature to obtain RuO$_2$ nanorods (NRs) hybrid MWCNTs. Then the hybrid material was used as a catalyst (*r*-RuO$_2$/MWCNT) for the aerial oxidation of alcohols and the result was found to be good.

Keywords: MWCNTs, RuO$_2$ nanostructures, Dry synthesis, Heterogeneous catalyst, Transfer hydrogenation, Aerial oxidation

1. Introduction

Catalytic reduction of carbonyl compounds (C=O) to their corresponding alcohols is an essential organic transformation in both industrial and fine chemical processes [1, 2]. There are several metal-based catalytic systems have long been proposed to perform this transformation [3, 4]. However, due to simple and cost effective protocol, most of the recent studies are focused on the transition metal-catalyzed transfer hydrogenation of carbonyl compounds by using 2–propanol (*i*-PrOH) as a hydrogen donor [5]. From an economical point of view, heterogeneous metal nanoparticles (MNPs) including ruthenium nanoparticles (RuNPs) have advantages over homogeneous catalysts due to their simple recovery and reusability [6, 7]. Particularly, RuNPs-supported catalysts have been widely employed for the reduction of carbonyl compounds due to their high activity, selectivity, versatility and reusability [8−10]. Kantam *et al*., [11] investigated MgO stabilized RuNPs catalyst for the transfer hydrogenation of carbonyl compounds. Yamaguchi *et al*., [12] prepared highly dispersed $Ru(OH)_x/TiO_2$ composite and used as a catalyst for the liquid-phase hydrogen transfer reactions. They found that the $Ru(OH)_x/TiO_2$ catalyst is highly effective and selective. In spite of higher catalytic activity, most of the common RuNPs (supported on metal oxide and polymeric materials) often exhibit less stability in high basic and acidic reaction conditions and, consequently, the reusability and selectivity of the catalyst are highly limited [13]. Therefore, developing an efficient and stable catalyst for the transfer hydrogenation of carbonyl compounds is still a challenging task.

Among the carbon building blocks (CNTs, fullerenes, graphene and carbon nanofibers), multiwall carbon nanotubes (MWCNTs) have played a significant role as a support in various fields including catalysis [14, 15]. In fact, MWCNTs have unique and superior properties such as chemical inertness, high stability and huge surface area [16]. Till date, several MWCNTs-

supported MNPs catalysts have been proposed. Particularly, MWCNTs-supported RuNPs has shown more versatility in carrying out the selective catalytic processes. Recently, Yu *et al*., [17] investigated the $RuO_2.xH_2O/CNT$ nanocatalysts for the aerobic oxidation of benzyl alcohol. Yang and co-workers [18] have prepared the RuNPs/MWCNT composite by 'wet synthesis' method and employed as a nanocatalyst for the oxidation of alcohols. They found that the RuNPs/MWCNT is highly effective, stable and reusable. However, in the common 'wet synthesis' method, several factors such as solvent, concentration of metal precursor, reducing agent, time and temperature need to be controlled carefully to obtain very good adhesion and homogeneous distribution of MNPs on MWCNTs [19–22]. Very recently, the solventless bulk synthesis so called 'dry synthesis' has been attracting greater interest due to its very simple protocol, better adhesion of MNPs on carbon materials, and has an advantage of least parameters to control [20]. In our very recent course of investigation, we prepared CuO/MWCNT [23], GNP-RuNRs [24], GNS-RuNPs [25] and RuO_2/SWCNT [26] by a simple 'dry synthesis' method. Also, we found that the resultant composites are highly active as nanocatalysts in the various organic transformations. Encouraged by these results, we presumed that the RuO_2/MWCNT composite prepared by 'dry synthesis' method would also exhibit a good catalytic activity for the reduction of carbonyl compounds. Herein, we report the 'dry synthesis' of RuO_2/MWCNT and its catalytic activity towards reduction of carbonyl compounds. Chemoselectivity, heterogeneity and stability of the RuO_2/MWCNT were also examined. The used catalyst was separated out from the reaction and reused in the same reaction as well as in the aerial oxidation of alcohols. The selective oxidation of alcohols is one of the very essential transformations in organic synthesis and also the oxygenated products are extremely valuable in chemical industries

4

[27−29]. Mainly, Ru-catalyzed aerial oxidation of alcohols has been attracting a great deal of attention due to its higher activity and selectivity [30−32].

2. Experimental

2.1. Materials and characterization

High purity MWCNTs with diameter ranging from 15 to 20 nm were used. The MWCNTs were produced in large scale through the optimal combination of chemical vapor deposition synthetic method, and subsequent thermal treatment at 2800°C in an argon atmosphere [33]. $Ru(acac)_3$ (97%), H_2SO_4 (98%), HNO_3 (70%) and HCl (70%) were purchased from Wako pure chemicals, Japan. All other chemicals were purchased from Aldrich and used as received.

The surface morphology of the RuO_2/MWCNT was investigated by TEM (JEM-2100 JEOL Japan) with accelerating voltage of 120 kV. The weight percentage and homogeneous distribution of RuO_2NPs in the RuO_2/MWCNT were confirmed by SEM-EDS [Hitachi (model-3000H) Scanning Electron Microscope]. The same field of view was then scanned using an EDS spectrometer to acquire a set of X-ray maps for Ru, C and O using 1 ms point acquisition for approximately one million counts. The interaction of RuO_2NPs with MWCNTs was examined by Raman spectrometer (Hololab 5000, Kaiser Optical Systems Inc., USA) using argon laser at 532 nm with a Kaiser holographic edge filter. WAXD experiments were performed at room temperature using a Rotaflex RTP300 (Rigaku Co., Japan) diffractometer at 50 kV and 200 mA. Nickel-filtered Cu Kα radiation ($10 < 2\theta < 80°$) was used for the measurements. To confirm the chemical state of Ru in the RuO_2/MWCNT, XPS spectrum was recorded in Kratos Axis-Ultra DLD model instrument. Before the XPS analysis, the sample (RuO_2/MWCNT) was irradiated

under Mg Kα ray source. The specific surface area of the RuO$_2$/MWCNT was measured by BET surface area analyzer (Micromeritics–Pulse Chemisorb 2700). Prior to the measurement, the sample was degassed for 2 h in N$_2$ atmosphere at 200°C by using the degassing unit [Micromeritics–Desorb 2300 A]. Shimadzu-2010 Gas chromatograph (GC) was used to analyze the reaction mixture.

2.2. Dry synthesis of RuO$_2$/MWCNT

In a typical experiment, 0.5 g of pure MWCNTs were chemically treated with a 3:1 mixture of conc. H$_2$SO$_4$ and conc. HNO$_3$, and then the mixture was sonicated at 40°C for 3 h in ultrasonic bath. After cooling to 25°C, the solution was diluted with 500 mL of deionized water and then vacuum-filtered through a filter paper of 0.65 μm porosity. The resultant solid mass (*f*-MWCNTs) was frequently washed with deionized water until the pH became neutral and then dried in *vacuo* at 60°C. Then, 0.13 g of Ru(acac)$_3$ was added into 0.5 g of *f*-MWCNTs and mixed well by a mortar and pestle. The homogeneous mixture of *f*-MWCNTs and Ru(acac)$_3$ was obtained in 13-15 minutes. Finally, the mixture was calcinated under N$_2$ atmosphere at 350°C for 3 h in a muffle furnace. Fig. 1 shows schematic illustration of the procedure for the preparation of RuO$_2$/MWCNT.

2.3. Transfer hydrogenation of carbonyl compounds

In a typical procedure, a 5 mg (0.77 mol%) of RuO$_2$/MWCNT and 80 mg (2 mmol) of NaOH were stirred with 5 mL of *i*-PrOH taken in an ace pressure tube equipped with a stirring bar. Then the substrate (1 mmol) was added to the stirring solution and then the mixture was heated at 82°C. The completion of the reaction was monitored by GC. After the reaction, the

catalyst was separated out from the reaction mixture by simple centrifugation and the products and unconverted reactants were analyzed by GC without any purification. Selectivity of the product for each reaction was also calculated. Finally, the separated RuO$_2$/MWCNT was washed well with diethyl ether followed by drying in an oven at 60°C for 5 h and it was reused for the subsequent transfer hydrogenation of carbonyl compounds to investigate the reusability of the RuO$_2$/MWCNT.

2.4. Aerial oxidation of alcohols

5 mg of *r*-RuO$_2$/MWCNT (0.68 mol%) was stirred with 3 mL of toluene taken in a round-bottomed flask equipped with a condenser and a magnetic stirrer. The substrate (1 mmol) was added to the stirring solution and then the mixture was refluxed at 110°C under atmospheric pressure of air. The completion of the reaction was checked by GC. After the reaction, the *r*-RuO$_2$/MWCNT was separated out from the reaction mixture by simple centrifugation and the products and unconverted reactants were analyzed by GC without any purification. Selectivity of the product for each reaction was also calculated.

2.5. Product confirmation and analysis

In order to confirm the formation of the product, samples of both reactant and products were dissolved in ethyl acetate and then analyzed by GC. GC was equipped with 5% diphenyl and 95% dimethyl siloxane, Restek-5 capillary column (0.32 mm dia, 60 m in length) and a flame ionization detector (FID). N$_2$ was used as a carrier gas. The initial column temperature was increased from 60 to 150°C at the rate of 10°C/min and then to 220°C at the rate of 40°C/min.

During the product analysis, the temperatures of the FID and injection port were kept constant at 150 and 250°C, respectively.

3. Results and discussion

3.1. Characterization of RuO₂/MWCNT

The surface morphology of the RuO_2/MWCNT was investigated in detail by using TEM analysis. Fig. 2 shows the TEM images [Fig. 2(i-v)] of RuO_2/MWCNT and the particle size-distribution histogram of RuO_2NPs [Fig. 2(vi)] in the RuO_2/MWCNT. As can be seen from Fig. 2(i-v), ultra fine and homogeneously dispersed RuO_2NPs were externally attached on the surface of MWCNTs with a very narrow particle size distribution. The size distribution histogram of RuO_2NPs [Fig. 2(vi)] confirmed that the diameter of RuO_2NPs ranges from 0.5 to 4 nm, with a mean diameter of 1.8 nm. Worth mentioning that there was no free RuO_2NPs were observed in the background of the TEM images [Fig. 2(iv-v)], which showed a complete utilization of the RuO_2NPs. Moreover, FE-SEM images (Fig. S1 in supporting information) were also taken for the RuO_2/MWCNT and found that a very small RuO_2NPs are well dispersed and externally attached on the surface of MWCNTs. Subsequently, the specific surface area of the RuO_2/MWCNT was determined by BET analysis. Interestingly, a high specific surface area of 189.3 m^2 g^{-1} with a pore volume of 0.898 cm^3 g^{-1} and a BJH desorption average pore diameter of 186.98 Å was found. In addition, the surface area per unit mass (S) of RuO_2NPs is calculated to be 478.1 m^2 g^{-1} based on the equation $S = 6000/(\rho \times d)$ [34], where d is the mean diameter, and ρ is the density of RuO_2 (6.97 g cm^{-3}).

In order to determine the weight percentage of Ru in RuO_2/MWCNT and to inspect the homogeneous distribution of RuO_2NPs on MWCNTs, SEM-EDS and their corresponding

8

elemental mapping images were taken for RuO_2/MWCNT (Fig. 3). The weight percentage of Ru in RuO_2/MWCNT was 7.97 wt%, as determined by EDS analysis [Fig. 3(ii)]. Fig. 3(iv) and (v) shows that the distribution of RuO_2NPs in RuO_2/MWCNT was homogeneous. As seen from Fig 3(iii), (iv) and (v), the RuO_2/MWCNT contains carbon, ruthenium and oxygen elements only; it indicates that the proposed method (dry synthesis) is reliable and effective.

XPS spectra were recorded for MWCNTs (**a**), *f*-MWCNTs (**b**) and RuO_2/MWCNT (**c**) to study the formation of oxygen functional groups on MWCNTs, and the chemical state of Ru in RuO_2/MWCNT (Fig. 4 and Fig. 5). As expected, all the three samples (**a**, **b** and **c**) demonstrated a C 1s peak and O 1s peak at 284.4 and 532.5 eV, respectively (Fig. S2 in supporting information). Referring Fig. 4(i), the binding energy (BE) of the C–C and C–H bonds was observed at 284.5–285 eV and the peaks at 285.1, 285.5, 286.6 and 288.5 eV were attributed to C–OH, –C–O–C–, C=O and –COOH groups, respectively [35]. Moreover, the deconvolution of O 1s spectra of *f*-MWCNTs [Fig. 4(ii)] resulted in five peaks located at 529.6, 530.7, 531.5, 532.2 and 533.5 eV, which were assigned to the C=O, –COOH, C–OH, –C–O–C– and H_2O respectively [36]. This result confirmed the successful creation of oxygen functional groups on the surface of MWCNTs. The two main reasons for the functionalization of MWCNTs are; (i) to make the MWCNTs hydrophilic for the homogenous decoration of RuO_2NPs on MWCNTs, and (ii) to create additional nucleation centers for the better adhesion of RuO_2NPs on MWCNTs. Moreover, these functional groups play a bridging role between the RuO_2NPs and MWCNTs; consequently, good dispersion and strong attachment of RuO_2NPs on MWCNTs were achieved [37]. The XPS spectrum of the RuO_2/MWCNT in Ru 3p region [Fig. 5(ii)] showed BE of Ru $3p_{3/2}$ at 462.5 eV and Ru $3p_{1/2}$ at 485.2 eV, which corresponded to the photoemission from RuO_2 (Ru^{4+}) [37]. In Fig. 5(i), the XPS spectrum of the RuO_2/MWCNT show Ru $3d_{5/2}$ peak at 280.8

eV which is also attributed to the photoemission from RuO_2 [37]. The overlapping of the C 1s and the Ru $3d_{3/2}$ peaks at ~285 eV makes it complicated to assign the BE of Ru $3d_{3/2}$ [Fig. 5(i)]. Fig. 6(i) shows the XRD patterns of RuO_2/MWCNT. The diffraction peaks were observed at 26.5° and 42.4°, corresponding to the (002) and (100) crystal planes of MWCNTs, respectively, which attributed to the hexagonal graphite structures of MWCNTs [24]. In addition to that, RuO_2/MWCNT showed signature patterns at 27.5°, 34.9°, 39.9° and 54.5° corresponding to the typical crystal faces (110), (101), (200) and (220) of RuO_2 (JCPDS 21-1172), respectively [24]. The broadness of the diffraction peaks confirmed that the RuO_2NPs in RuO_2/MWCNT are in nanocrystalline nature.

The nature of interaction between RuO_2NPs and MWCNTs was investigated by comparing the Raman spectra of *f*-MWCNTs (**a**) and RuO_2/MWCNT (**b**) [Fig. 6(ii)]. As expected, samples **a** and **b** showed two characteristic peaks at 1345 and 1580 cm^{-1}, corresponding to the sp^3- and sp^2-hybridized carbons which authenticated the disordered graphite (D band) and the ordered state graphite (G band) of MWCNTs [38]. Well known that, the ratio of D and G bands (I_D/I_G) intensities is often used as a diagnostic tool to evaluate the defect concentration in MWCNTs. Therefore, I_D/I_G was calculated for the samples **a** and **b** [Fig. 6(ii)]. The data revealed that RuO_2NPs were strongly attached on the surface of MWCNTs as the I_D/I_G ratio was reasonably high for RuO_2/MWCNT (1.4579) in comparison to that of *f*-MWCNTs (1.4113). In addition, negative shift was also observed in the D band (1347 to 1341 cm^{-1}) and G band (1580 to 1576 cm^{-1}) for RuO_2/MWCNT, which indicates that RuO_2NPs interacted strongly on the surface of the MWCNTs [39]. Worth mentioning that, the absence of peaks around 1700 cm^{-1} in the Raman spectra of **a** and **b** suggested that the present process produces fairly pure MWCNTs.

3.2. Optimization of reaction conditions

In order to get an effective conversion of carbonyl compounds to alcohols, reaction parameters such as base, amount of base, amount of catalyst, temperature and reaction time were optimized (Table 1). The conversion of acetophenone (model substrate) was checked through GC. At first, transfer hydrogenation of acetophenone was investigated with different bases such as KOH, NaOH, K_2CO_3 or $(CH_3)_3COK$. Among them, NaOH was found to be the efficient since it gave an excellent yield of 96% (Table 1, entries 1-4). The amount of base also played a crucial role in the present RuO_2/MWCNT system (Table 1, entries 2, 5-7); a 2 mmol of base was required to achieve the excellent yield (Table 1, entry 2). Similarly, the amount of catalyst was optimized; as a consequence, a very lower conversion of 13% was obtained in the absence of RuO_2/MWCNT (Table 1, entry 8). Whereas addition of 5.0 mg (0.71 mol%) of RuO_2/MWCNT yielded 96% of the product (Table 1, entry 2). Lesser amount of catalyst (2.5 mg; 0.24 mol%) was ineffective (27%) (Table 1, entry 9) which may be due to the presence of insufficient number of active sites (RuO_2) for the substrates. Furthermore, increase of the amount of the catalyst (7.5 and 10 mg; 0.48 and 0.96 mol%) showed no significant change in the yield (Table 1, entries 10-11). Hence, 5.0 mg (0.77 mol%) was found to be the optimum amount of the catalyst. Subsequently, reaction temperature was optimized. At the lower reaction temperatures (27, 50 and 70°C), the reactions were very slow, which gave very poor yield (Table 1, entries 12-14). But excellent yield was obtained (96%) when the reaction is stirred at the temperature of 82°C (Table 1, entry 2). This might be due to faster adsorption of the substrates on RuO_2 active sites at 82°C. Progress of the reaction was monitored at every 10 min time interval (Table 1, entries 15-23). No further increase in the yield after 45 min concluded that 45 min is the optimum reaction time (Table 1, entry 2). Worth mentioning that under the optimized reaction conditions, the

present RuO$_2$/MWCNT system achieved an excellent yield of 96% with a good turnover number of 125 and turnover frequency of 167 h^{-1}. The optimized reaction conditions were adopted to extend the substrate scope.

3.3. Extension of scope

Benzaldehyde, substituted benzaldehydes and other substituted aldehydes were converted into the corresponding primary alcohols in excellent to moderate yields (Table 2, entries 1-10). The yield of the products was moderately affected by the substituent on the aromatic ring, but the selectivity was maintained. Initially, benzaldehyde was converted into 95% of benzyl alcohol with 100% selectivity after 45 min (Table 2, entry 1). But HSi(OMe)$_3$/LiOMe catalytic system yielded only 85% of benzyl alcohol even after 20 h [40]. Electron withdrawing substituent in the phenyl ring retarded the reactivity. In evidence to this, 4-bromo (Table 2, entry 2), 2-bromo (Table 2, entry 3), 4-chloro (Table 2, entry 4) and 4-nitro benzaldehydes (Table 2, entry 6) were found to be less reactive compared to unsubstituted benzaldehyde in the present catalytic system. In contrast, the electron releasing substituent increased the reactivity. For example, 4-methylbenzaldehyde was hydrogenated to form 4-methylbenzyl alcohol in 97% yield with 100% selectivity (Table 2, entry 5). Aldehydes with bulky substituent namely 2-naphthaldehyde and 1-pyrenecarboxaldehyde were reduced to corresponding primary alcohols with lesser selectivity (82 and 80%). The former one was converted into 2-naphthalenemethanol (51%) after 45 min (Table 2, entry 7), whereas the later required 120 min to achieve 54% of the corresponding reduced product (Table 2, entry 8). 100% selectivity was achieved when 3-phenylpropanal was hydrogenated to 3-phenylpropan-1-ol after 120 min (Table 2, entry 9). *N,N*-Dimethyl

benzaldehyde yielded 75% of *N*,*N*-dimethylbenzyl alcohol after 45 min with 95% selectivity (Table 2, entry 10).

After the successful reduction of aldehydes to primary alcohols, ketones were converted into secondary alcohols under the same reaction conditions (Table 2, entries 1-15). Acetophenone was hydrogenated to 1-phenylethanol (96%) with 100% selectivity after 45 min (Table 3, entry 1). But $HSi(OMe)_3$/$LiOCMe_2CMe_2OLi$ [40] and Au/TiO_2 catalytic systems [41] required 20 and 4 h respectively for the complete reduction of acetophenone. In contrast to the reduction of benzaldehydes, acetophenones bearing electron withdrawing or electron releasing substituent in the phenyl ring yielded the corresponding substituted 1-phenylethanol more readily. In witness to this statement, 4-bromoacetophenone and 4-methoxyactophenone were converted into their corresponding secondary alcohols namely 4-bromo-1-phenylethanol (Table 3, entry 2) and 4-methoxy-1-phenylethanol (Table 3, entry 3) in 92 and 88% yield respectively with excellent selectivity after 45 min. But RuCs-β(IMP-carbonyl) catalyst yielded 98% of 4-bromo-1-phenylethanol and 92% of 4-methoxy-1-phenylethanol only after 48 and 36 h respectively [42]. Acetophenones having substituent at the *ortho*, *meta* or *para* position were also subjected to transfer hydrogenation. 3-Nitroacetophenone (Table 3, entry 4), 2-methylacetopheone (Table 3, entry 5) and 4-methylacetophone (Table 3, entry 6) produced corresponding 1-phenylethanol with excellent conversion, selectivity and yield. Particularly, in the reduction of 2-methylacetopheone to 1-(*o*-tolyl)ethanol (Table 3, entry 5), the present catalytic system gave a better yield of 95% (100% selectivity) with an excellent TON (123) and TOF (148 h^{-1}) values after only 50 min. Whereas Ru(OH)$_x$/TiO_2 system gave 82% (with TON/TOF of 82/27 h^{-1}) of the same product only after 3 h even at 90°C under Ar atmosphere [12]. Substituted benzophenone specifically 4-methoxybenzophenone was reduced to 4-methoxydiphenylmethanol (73%) after

45 min (Table 3, entry 7); moderate yield of the product may be due to the presence of the bulky substituent [43]. Scope of this system was also extended to aliphatic and alicyclic carbonyl compounds. Aliphatic ketones yielded the corresponding alcohols in good to excellent yields. Almost 100% selectivity was achieved in all the cases with the yield ranging from 95 to 98% (Table 3, entries 8-10). Notably, in the reduction of less reactive 2-butanone to 2-butanol (Table 3, entry 8), the present RuO_2/MWCNT system showed a better yield of 95% (100% selectivity) when compared to GNPs-RuO_2NRs system [24]. The better yield is due to the higher surface area of RuO_2/MWCNT (189.3 m^2 g^{-1}) than the GNPs-RuO_2NRs (65.17 m^2 g^{-1}). Similarly, 2-octanone gave 2-octanol in an excellent yield of 98% (100% selectivity) just after 1 h (Table 3, entry 11) whereas $Ru(OH)_x$/TiO_2 system exhibited 92% yield even after 2 h [12]. In contrast to Fe@SiO_2Ru nanocatalyst [44], alicyclic alcohols with different ring size were produced from the alicyclic ketones with 100% selectivity, but they took longer reaction times. As the ring size increases, decreased reactivity was observed (Table 3, entries 12-14). The reactivity order is cyclohexanone (92%) > cycloheptanone (88%) > cyclododecanone (77%). But nickel/aluminosilicate catalyst yielded only 58% of cyclohexanone under similar reaction conditions [45]. 100% Selectivity was accomplished when carbonyl functionality was present in the side chain of the alicyclic ring (Table 3, entry 15).

In order to illustrate the synthetic utility of the present catalytic system, some heterocyclic aldehydes and ketones were subjected to transfer hydrogenation (Table 4). 2-Acetylthiophene yielded the corresponding alcohol (97%) after 90 min with 100% selectivity (Table 4, entry 1). RhCl(PPh$_3$)$_3$ catalytic system gave only 4% of the same product [46]. Likewise, the present system was found to be effective in the reduction of 2-furfuraldehyde which gave 74% of the product (Table 4, entry 2). Only 50% of the product was achieved from the reduction of 2-

furfuraldehyde with Pt decorated Al_2O_3 catalyst [47]. 3-Formylindol and 5-formylindol were effectively reduced to indole-3-methanol (88%) and indole-5-methanol (96%) respectively with very good selectivity (Table 4, entries 3 and 4). In the same way 4-(2-pyridyl)benzaldehyde gave 77% of 4-(2-pyridyl)benzyl alcohol with 100% selectivity after 100 min (Table 4, entry 5). Worth mentioning that RuO_2/MWCNT system achieved good yields (51 to 98%) with high TON (127 to 66) and TOF (246 to 35 h^{-1}) values in the transfer hydrogenation of carbonyl compounds.

3.4. Chemoselectivity of RuO₂/MWCNT

Referring table 4, the present RuO_2/MWCNT catalytic system is highly chemoselective in nature. 4-Acetylbenzaldehyde was chemoselectively reduced to 1-(4-(hydroxymethyl)phenyl)ethanone (Table 5, entry 1). The phenyl ring containing aldehyde and ester functional groups was subjected to transfer hydrogenation and only the aldehyde was selectively reduced to primary alcohol without affecting the ester functionality (Table 5, entry 2). Similar trend was observed with the phenyl ring having ketone and acid functional groups (Table 5, entry 3).

3.5. Effect of particle size on catalytic activity

Particle size and surface area are important factors in any nanocatalytic system. In order to determine the effect of the RuO_2 particle size on catalytic efficiency in terms of yields, another catalyst with RuO_2 particle size of around 5 to 12 nm (b-RuO_2/MWCNT) was prepared by calcinating the mixture [f-MWCNT and Ru(acac)$_3$] under air atmosphere at 375°C for 3 h and its catalytic performance was compared with the RuO_2/MWCNT. At first, b-RuO_2/MWCNT nanocatalyst was characterized by TEM analysis. It was found that the particle size of RuO_2NPs

was around 5 to 12 nm with the mean diameter of 9 nm [Fig. 7(i) and (ii)]. The weight percentage of Ru in b-RuO$_2$/MWCNT was found to be 8.01 by using SEM-EDS analysis [Fig. 7(iii)]. XPS analysis revealed that Ru was present as RuO$_2$ and hence it showed 3p$_{1/2}$ peak at 485 eV and 3p$_{3/2}$ peak at 462 eV. The surface area per unit mass (S) of b-RuO$_2$/MWCNT was found to be 88.6 m^{2}g^{-1}. After the characterization, b-RuO$_2$/MWCNT was used as a catalyst for the transfer hydrogenation of some carbonyl compounds (Table 6). Acetophenone was reduced to 1-phenylethanol in moderate yield of 65% (Table 6, entry 1) whereas the RuO$_2$/MWCNT system gave an excellent yield (96%) of the desired product (Table 3, entry 1). The reactivity of aliphatic carbonyl compounds was found to be lesser in the b-RuO$_2$/MWCNT system (Table 6, entry 2) when compared to RuO$_2$/MWCNT system. Similarly, reduction of alicyclic ketone produced lower yield of alicyclic alcohol with b-RuO$_2$/MWCNT catalyst (Table 6, entry 3). Same kind of behavior was observed with benzaldehyde (Table 6, entry 4) and heterocyclic carbonyl compound (Table 6, entry 5). Hence, it is inferred that the excellent activity of RuO$_2$/MWCNT compared to b-RuO$_2$/MWCNT was mainly due to the ultra-fine structure of the RuO$_2$NPs.

3.6. Heterogeneity and reusability of RuO$_2$/MWCNT

In order to understand the heterogeneous nature of the RuO$_2$/MWCNT, a hot filtration test was performed. In a typical test, reduction of acetophenone was carried out under optimized conditions for 20 min and the yield of 1-phenylethanol determined by GC was 45%. Subsequently, the RuO$_2$/MWCNT was filtered out from the reaction mixture (after 20 min) and then the reaction was continued without the catalyst for 60 min. The progress of the reaction was monitored at each 10 min intervals; the results are shown in Fig. 8(i). It can be seen that there

16

was no significant change in the yield in the absence of the catalyst even after extended reaction time (after 60 min), which indicated that the reaction proceeded mainly due to the catalytic effect of RuO_2/MWCNT and also there was no leaching of Ru from the RuO_2/MWCNT.

Since reusability is one of the important features of the nanocatalysts, it was also tested for the RuO_2/MWCNT. After the first cycle, the catalyst was separated out from the reaction mixture by simple centrifugation, washed well with diethyl ether, dried at 150°C, and then reused in the second cycle. Likewise, the catalytic cycle was repeated for 8 times and the yield monitored by GC is shown in Fig. 8(ii). Interestingly, the RuO_2/MWCNT system gave an excellent yield of 87% (100% selectivity) with high TON (113) and TOF (151 h^{-1}) values at the 8th cycle, which indicated its good reusability. Moreover, the reused catalyst (u-RuO_2/MWCNT) was further investigated by TEM, SEM-EDS and XPS analyses (Fig. S3 in supporting information). In comparison to the fresh RuO_2/MWCNT, no significant change in the morphology, size, shape, chemical state and weight percentage of Ru was observed for the u-RuO_2/MWCNT. Hence, it is obvious that the RuO_2/MWCNT is physically as well as chemically stable.

3.7. Versatility of RuO$_2$/MWCNT

Inspired by the high stability of the RuO_2/MWCNT, the u-RuO_2/MWCNT was further applied in oxidation reactions. Initially, the u-RuO_2/MWCNT was washed with diethyl ether and dried in an oven at 60°C for 5 h. Then the washed u-RuO_2/MWCNT was calcinated under N_2 atmosphere at 450°C for 6 h in a muffle furnace to obtain ruthenium oxide nanorods (RuO_2NRs) hybrid MWCNTs. The resultant hybrid (r-RuO_2/MWCNT) was well characterized and it was used as a catalyst for the aerial oxidation of alcohols. Fig. 9 shows the TEM images [Fig. 10(i-

iii)], SEM and the corresponding EDS spectrum [Fig. 10(iv) and (v)] and XPS spectrum [Fig. 10(vi)] of *r*-RuO$_2$/MWCNT. The TEM images confirmed the external attachment of very fine and well dispersed RuO$_2$NRs on the MWCNTs. The length and diameter of RuO$_2$NRs were found in the range of 20-40 and 7-14 nm, respectively. The weight percentage of Ru in the *r*-RuO$_2$/MWCNT was found to be 6.92 from SEM-EDS analysis. In the XPS spectrum of *r*-RuO$_2$/MWCNT [Fig. 10(vi)], the BE of Ru 3p$_{3/2}$ at 462.4 eV and Ru 3p$_{1/2}$ at 485.1 eV were attributed to the photoemission from RuO$_2$ (Ru^{4+}) [48]. It was found that the *r*-RuO$_2$/MWCNT is highly efficient for the aerial oxidation of alcohols (Table 7). In the preliminary test, fortunately, 1-phenylethanol showed a very high conversion of 98% with 100% selectivity (Table 7, entry 1). Inspired by this result, the scope of the catalytic system was extended to a wide range of aromatic, aliphatic, alicyclic and heterocyclic alcohols (Table 7). Benzyl alcohol was converted into benzaldehyde in 91% yield (94% selectivity) without any over oxidation to benzoic acid (Table 7, entry 2). Cu/AlO(OH) catalytic system took 7 h for the complete oxidation of benzyl alcohol even in presence of a strong oxidizing agent (H$_5$IO$_6$) [49]. In the oxidation of less reactive 2-octanol, the present catalytic system gave a better yield of 78% with 100% selectivity compared to RuO$_2$-FAU catalytic system (Table 7, entry 3) [28]. Moreover, less reactive cyclopentanol was also converted into cyclopentanone in better yield of 70% whereas Au/Fe$_3$O$_4$@SiO$_2$-catalyzed reaction gave only 42% yield (Table 7, entry 4) [50]. The *r*-RuO$_2$/MWCNT catalytic system showed comparatively lesser yields when compared with the commercial Ru/Al$_2$O$_3$ catalytic system [30]. Interestingly, the *r*-RuO$_2$/MWCNT catalytic system was also adopted for the heterocyclic alcohols. For example, 1-furyl ethanol yielded 1-furylethanone in 62% yield with a moderate selectivity of 80% (Table 7, entry 5). The results

concluded that the *r*-RuO$_2$/MWCNT effectively catalyzed oxidation of various alcohols; this confirmed that the proposed catalyst (RuO$_2$/MWCNT) was stable and highly versatile.

4. Conclusions

In summary, a very simple 'dry synthesis' method was used to decorate the RuO$_2$NPs on MWCNTs. The RuO$_2$/MWCNT catalyst exhibited excellent catalytic activity, chemoselectivity, stability, heterogeneity and reusability in the transfer hydrogenation of carbonyl compounds. Interestingly, the present RuO$_2$/MWCNT system tolerated a wide range of functional groups. The excellent yield of the products is mainly due to the smaller particle size of the RuO$_2$NPs. Moreover, the versatility of the RuO$_2$/MWCNT was realized from the excellent activity of *r*-RuO$_2$/MWCNT catalyst in the aerial oxidation of alcohols.

References

[1]   G. Zassinovich, G. Mestroni, S. Gladiali, Chem. Rev. 92 (1992) 1051–1069.

[2]   D.A. Evans, S.G. Nelson, M.R. Gagne, A.R. Muci, J. Am. Chem. Soc. 115 (1993) 9800–9801.

[3]   R. Noyori, S. Hashiguchi, Acc. Chem. Res. (30) 1997 97–102.

[4]   R.A.W. Johnstone, A.H. Wilby, Chem. Rev. 85 (1985) 129–170.

[5]   B. Gottfried, J.N. Terry, Chem. Rev. 74 (1974) 567–580.

[6]   M. Shiding, L. Zhimin, H. Buxing, H. Jun, S. Zhenyu, Z. Jianling, J. Tao, Angew. Chem. Int. Ed. 45 (2006) 266–269.

[7]   B.F.G. Johnson, Coord. Chem. Rev. 190–192 (1999) 1269–1285.

[8]   I. Arindam, M. Niladri, M. Prasenjit, B. Sumit, K.L. Goutam, J. Catal. 284 (2011) 176–183.

[9]   L. Fang, L. Jing, X. Jie, J. Mol. Catal. A: Chem. 271 (2007) 6–13.

[10] B. Baruwati, V. Polshettiwar, R.S Varma, Tetrahedron Lett. 50 (2009) 1215–1218.

[11]   M.L. Kantam, R.S. Reddy, U. Pal, B. Sreedhar, S. Bhargavab, Adv. Synth. Catal. 350 (2008) 2231–2235.

[12] K. Yamaguchi, T. Koike, J.W. Kim, Y. Ogasawara, N Mizuno, Chem. Eur. J. 14 (2008) 11480–11487.

[13] E. Auer, A. Freund, J. Pietsch, T. Tacke, Appl. Catal. A: Gen. 173 (1998) 259–271.

[14] S. Philippe, C. Eva, Chem. Cat. Chem. 2 (2010) 1–47.

[15] S. Philippe, C. Massimiliano, K. Philippe, Appl. Catal. A: Gen. 253 (2003) 337–358.

[16] J.M. Planeix, N. Coustel, B. Coq, V. Bretons, P.S. Kumbhar, R.D.P. Geneste, P. Bernier, P.M. Ajayan, J. Am. Chem. Soc. 116 (1994) 7935–7936.

[17] H. Yu, X. Fu, C. Zhou, F. Peng, H. Wang, J. Yang, Chem. Commun. (2009) 2408–2410.

[18] X. Yang, X. Wang, J. Qiu, Appl. Catal. A: Gen. 382 (2010) 131–137.

[19] X.R. Ye, Y. Lin, C. Wang, M.H. Engelhard, Y. Wang, C.M. Wai, J. Mater. Chem. 14 (2004) 908–913.

[20] B. Wu, Y. Kuang, X. Zhang, J. Chen, Nano Today 6 (2011) 75–90.

[21] T. Vassilios, G. Vasilios, O. Eudokia, K. Michael, P. Dimitrios, Carbon 44 (2006) 848–853.

[22] Y. Lin, K.A. Watson, M.J. Fallbach, S. Ghose, J.G. Smith, D.M. Delozier, W. Cao, R.E. Crooks, J.W. Connell, ACS Nano 3 (2009) 871–884.

[23] M. Gopiraman, S. Ganesh Babu, Z. Khatri, W. Kai, Y.A. Kim, M. Endo, R. Karvembu, I.S. Kim, Carbon 62 (2013) 135–148.

[24] M Gopiraman, S. Ganesh Babu, Z. Khatri, K. Wei, E. Morinobu, R. Karvembu, I.S. Kim, Catal. Sci. Technol. 3 (2013) 1485–1489.

[25] M. Gopiraman, S.Ganesh Babu, Z. Khatri, K. Wei, Y.A. Kim, M. Endo, R. Karvembu, I.S. Kim, J. Phys. Chem. C 117 (2013) 23582–23596.

[26] M. Gopiraman, R. Karvembu, I. S. Kim, ACS Catal. 4 (2014) 2118–2129.

[27] W. E. Billups, B.E. Arney, L.J. Lin, J. Org. Chem. 49 (1984) 3436–3437.

[28] B.Z. Zhan, A. Thompson, Tetrahedron 60 (2004) 2917−2935.

[29] B. Michele, G. Pierre, Catal. Today 57 (2000) 127–141.

[30] K. Yamaguchi, N. Mizuno, Chem. Eur. J. 9 (2003) 4353–4361.

[31] B.Z. Zhan, M.A. White, T.K. Sham, J.A. Pincock, R.J. Doucet, K.V. Ramana Rao, K.N. Robertson, T.S. Cameron J. Am. Chem. Soc. 125 (2003) 2195–2199.

[32]   D.V. Bavykin, A.A. Lapkina, P.K. Plucinski, J.M. Friedrich, F.C. Walsh, J. Catal. 235 (2005) 10–17.

[33]   G.G. Wildgoose, C.E. Banks, R.G. Compton, Small 2 (2006) 182–93.

[34]   J. Lu, I. Do, L.T. Drzal, R.M. Worden, I. Lee, ACS Nano 2 (2008) 1825–1832.

[35]   O. Akhavan, Carbon 48 (2010) 509–519.

[36]   T. Kuila, S. Bhadra, D. Yao, N.H. Kim, S. Bose, J.H. Lee, Prog. Polym. Sci. 35 (2010) 1350–1375.

[37]   N. Chakroune, G. Viau, S. Ammar, L. Poul, D. Veautier, M.M. Chehimi, C. Mangeney, F. Villain, F. Fievet, Langmuir 21 (2005) 6788–6796.

[38]   M.S. Dresselhaus, G. Dresselhaus, R. Saito, A. Jorio, Phys. Rep. 409 (2005) 47–99.

[39]   A.G. Souza Filho, V. Meunier, M. Terrones, B.G. Sumpter, E.B. Barros, F. Villalpando-Paez, J.M. Filho, Y.A. Kim, H. Muramatsu, T. Hayashi, M. Endo, M.S. Dresselhaus, Nano Lett. 7 (2007) 2383–2388.

[40]   A. Hosomi, H. Hayashida, S. Kohra, Y.J. Tominaga, J. Chem. Soc. Chem. Commun. 1986 (1986) 1411−1412.

[41]   S.Z. Fang, H. Lin, N. Ji, C. Yong, H.Y. He, F.N. Kang, Chem. Commun. (2008) 3531−3533.

[42]   M.L. Kantam, B.P.C. Rao, B.M. Choudary, B. Sreedhar, Adv. Synth. Catal. 348 (2006) 1970–1976.

[43]   R. Noyori, T. Ohkuma, Angew. Chem. Int. Ed. 40 (2001) 40−73.

[44]   R.B. Nasir Baig, R.S. Varma, ACS Sust. Chem. Eng. 1 (2013) 805−809.

[45]   N. Neelakandeswari, G. Sangami, P. Emayavaramban, S. Ganesh Babu, R. Karvembu, N. Dharmaraj, J. Mol. Catal. A: Chem. 356 (2012) 90–99.

[46] K. Bogar, P. Krumlinde, Z. Bacsik, N. Hedin, J.E. Backvall, J.R. Ruiz, C.J. Sanchidrian, J.M. Hidalgo, J.M. Marinas, Eur. J. Org. Chem. 2011 (2011) 4409−4414.

[47] J. Kijenski, P. Winiarek, T. Paryjczak, A. Lewicki, A. Mikołajska, Appl. Catal. A: Gen. 233 (2002) 171−182.

[48] M. Gopiraman, H. Bang, S. Ganesh Babu, K. Wei, R. Karvembu, I.S. Kim, Catal. Sci. Technol. 4 (2014) 2099−2106.

[49] S. Ganesh Babu, P.A. Priyadarsini, R. Karvembu, Appl. Catal. A: Gen. 392 (2011) 218–224.

[50] R.L. Oliveira, P.K. Kiyohara, L.M. Rossi, Green Chem. 12 (2010) 144–149.

Table 1

Optimization of the reaction conditions for the transfer hydrogenation of acetophenone[a].
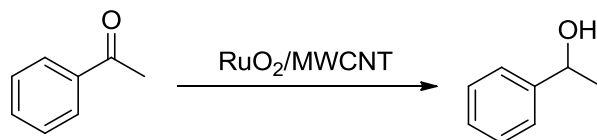
entry	base[b]	amount of base (mmol)	amount of catalyst (mol%)	temperature (°C)	time (min)	yield[c] (%)	TON/ (TOF h^{-1})[d]
1	KOH	2	0.77	82	45	26	34/45
2	**NaOH**	**2**	**0.77**	**82**	**45**	**96**	**125/167**
3	K$_2$CO$_3$	2	0.77	82	45	15	20/27
4	(CH$_3$)$_3$COK	2	0.77	82	45	39	51/68
5	NaOH	1	0.77	82	45	41	53/71
6	NaOH	1.5	0.77	82	45	56	73/97
7	NaOH	2.5	0.77	82	45	96	125/167
8	NaOH	2	0	82	45	11	-
9	NaOH	2	0.24	82	45	27	112/149
10	NaOH	2	0.48	82	45	49	102/136
11	NaOH	2	0.96	82	45	96	100/133
12	NaOH	2	0.77	25	45	15	20/27
13	NaOH	2	0.77	50	45	37	48/64
14	NaOH	2	0.77	70	45	52	68/91
15	NaOH	2	0.77	82	0	0	-
16	NaOH	2	0.77	82	10	29	38/224
17	NaOH	2	0.77	82	20	45	58/77
18	NaOH	2	0.77	82	30	59	77/154
19	NaOH	2	0.77	82	40	78	101/151
20	NaOH	2	0.77	82	60	96	125/125
21	NaOH	2	0.77	82	70	96	125/107
22	NaOH	2	0.77	82	80	97	126/95
23	NaOH	2	0.77	82	90	97	126/84

[a] All the reactions were performed with 1.0 mmol (117.0 µL) of acetophenone. [b] A 5 mL aliquot of i-PrOH was used in all the reactions. [c] GC yield. [d] TON/TOF [TON = the amount of product (mol) / the amount of active sites; TOF = TON/time (h)].

Table 2

RuO$_2$/MWCNT-catalyzed transfer hydrogenation of aldehydes[a].
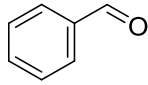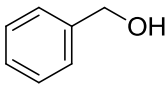
entry	substrate	product	time (min)	conv.[b] (%)	sel.[b] (%)	yield[b] (%)	TON/ (TOF h^{-1})
1			45	95	100	95	123/160
2			45	88	91	79	103/134
3			45	76	100	76	99/129
4			45	63	88	51	66/86
5			45	97	100	97	126/167
6			45	79	100	79	103/134
7			45	69	82	51	66/86
8			120	74	80	54	70/35
9			120	89	100	89	116/58
10			45	80	95	75	97/126
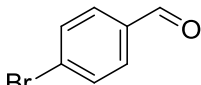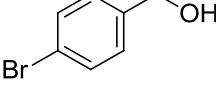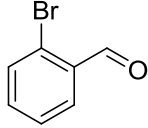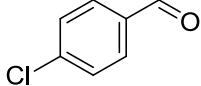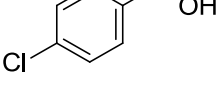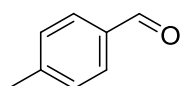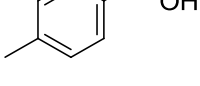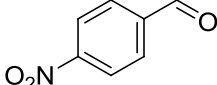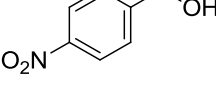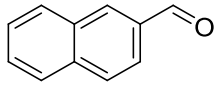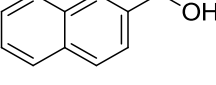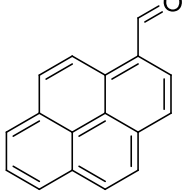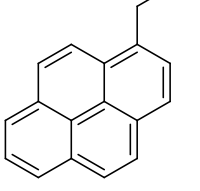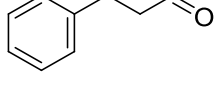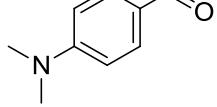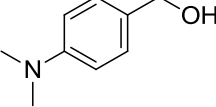
[a] Reaction conditions: Substrate (1 mmol), RuO_2/MWCNT (0.77 mol%), NaOH (2 mmol), i-PrOH (5 mL), 82°C. [b] Determined by GC analysis.

Table 3

RuO_2/MWCNT-catalyzed transfer hydrogenation of ketones[a].
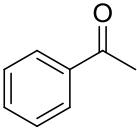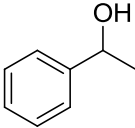
entry	substrate	product	time (min)	conv.[b] (%)	sel.[b] (%)	yield[b] (%)	TON/ (TOF h^{-1})
1			45	96	100	96	125/167
2			45	95	97	92	120/160
3			45	88	100	88	114/152
4			45	81	86	67	87/116
5			50	95	100	95	123/148
6			45	91	100	91	118/157
7			45	86	87	73	95/127
8			30	97	98	95	123/246
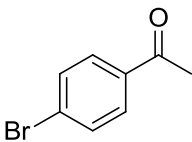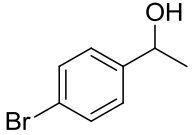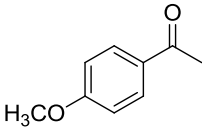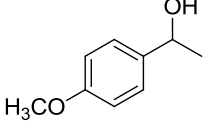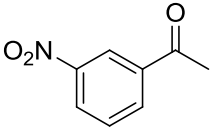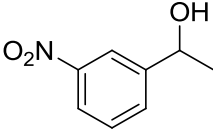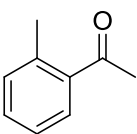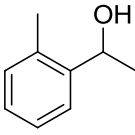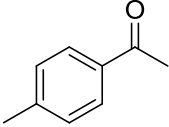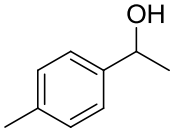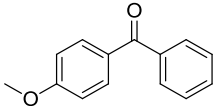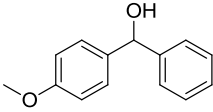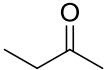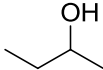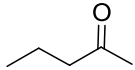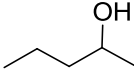
9			45	97	98	95	123/164
10			45	97	100	97	126/168
11			60	98	100	98	127/127
12			90	96	96	92	120/80
13			90	88	100	88	114/76
14			120	77	100	77	100/50
15			90	74	100	74	96/64
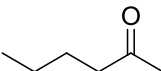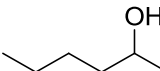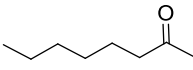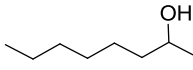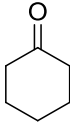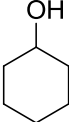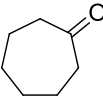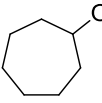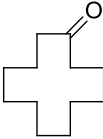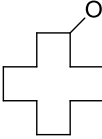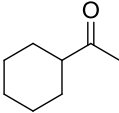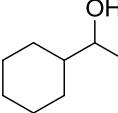
[a] Reaction conditions: Substrate (1 mmol), RuO_2/MWCNT (0.77 mol%), NaOH (2 mmol), i-PrOH (5 mL), 82°C. [b] Determined by GC analysis.

27

Table 4

RuO$_2$/MWCNT-catalyzed transfer hydrogenation of heterocyclic carbonyl compounds[a].
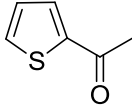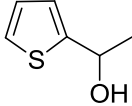
entry	substrate	product	time (min)	conv.[b] (%)	sel.[b] (%)	yield[b] (%)	TON/ (TOF h^{-1})
1			90	97	100	97	126/84
2			90	78	96	74	96/64
3			120	95	93	88	114/57
4			100	96	100	96	125/75
5			100	77	100	77	100/60
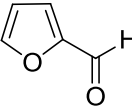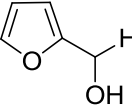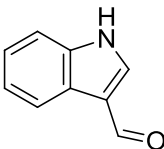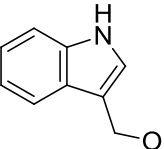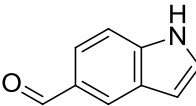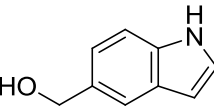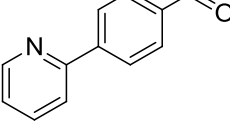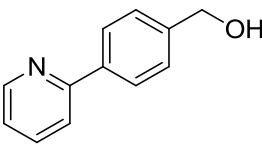
[a] Reaction conditions: Substrate (1 mmol), RuO$_2$/MWCNT (0.77 mol%), NaOH (2 mmol), *i*-PrOH (5 mL), 82°C. [b] Determined by GC analysis.

Table 5

Chemoselective transfer hydrogenation of carbonyl compounds catalyzed by RuO$_2$/MWCNT[a].
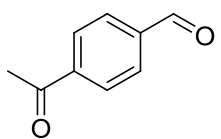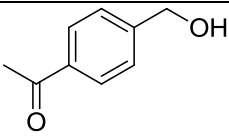
entry	substrate	product	time (min)	conv.[b] (%)	sel.[b] (%)	yield[b] (%)	TON/ (TOF h^{-1})
1			45	80	84	64	83/111
2			45	79	100	79	103/137
3			60	77	100	77	100/100
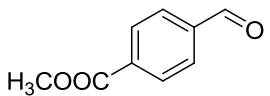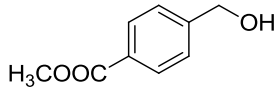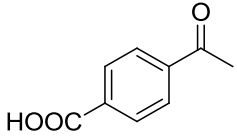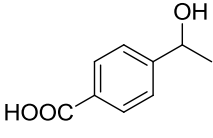
[a] Reaction conditions: Substrate (1 mmol), RuO$_2$/MWCNT (0.77 mol%), NaOH (2 mmol), i-PrOH (5 mL), 82°C. [b] Determined by GC analysis.

Table 6

Catalytic activity of *b*-RuO$_2$/MWCNT in the transfer hydrogenation of carbonyl compounds[a].
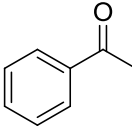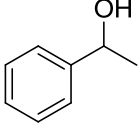
entry	substrate	product	time (min)	conv.[b] (%)	sel.[b] (%)	yield[b] (%)	TON/ (TOF h^{-1})
1			45	65	100	65	84/112
2			60	55	94	49	64/64
3			120	47	100	47	61/31
4			60	72	100	72	94/94
5			120	39	92	31	40/20
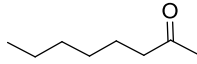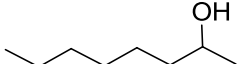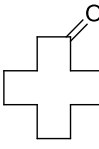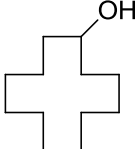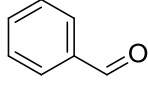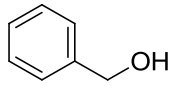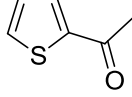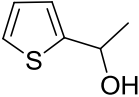
[a] Reaction conditions: Substrate (1 mmol), RuO$_2$/MWCNT (0.78 mol%), NaOH (2 mmol), *i*-PrOH (5 mL), 82°C. [b] Determined by GC analysis.

Table 7

Oxidation of alcohols catalyzed by *r*-RuO$_2$/MWCNT[a].

Entry	substrate	product	time (h)	conv.[b] (%)	sel.[b] (%)	yield[b] (%)
1			18	98	100	98
2			12	97	94	91
3			16	78	100	78
4			20	79	91	70
5			20	82	80	62
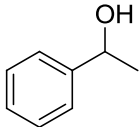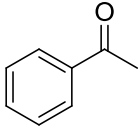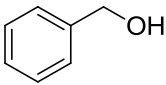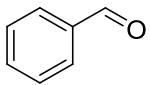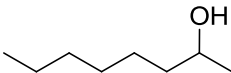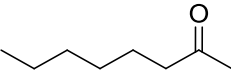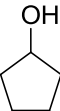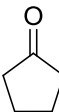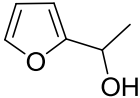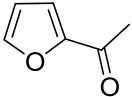
[a] Reaction conditions: Substrate (1 mmol), *r*-RuO$_2$/MWCNT (0.68 mol%), toluene (3 mL), 110°C. [b] Determined by GC analysis.
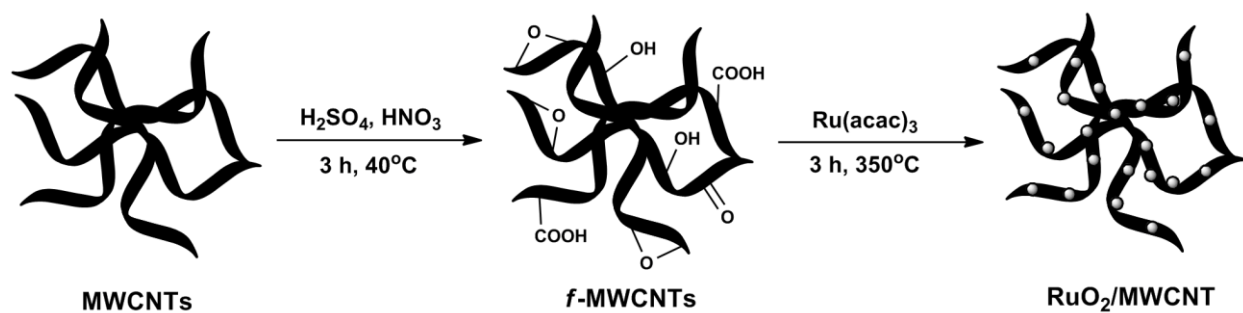
Fig. 1. Schematic illustration for the preparation of RuO_2/MWCNT.
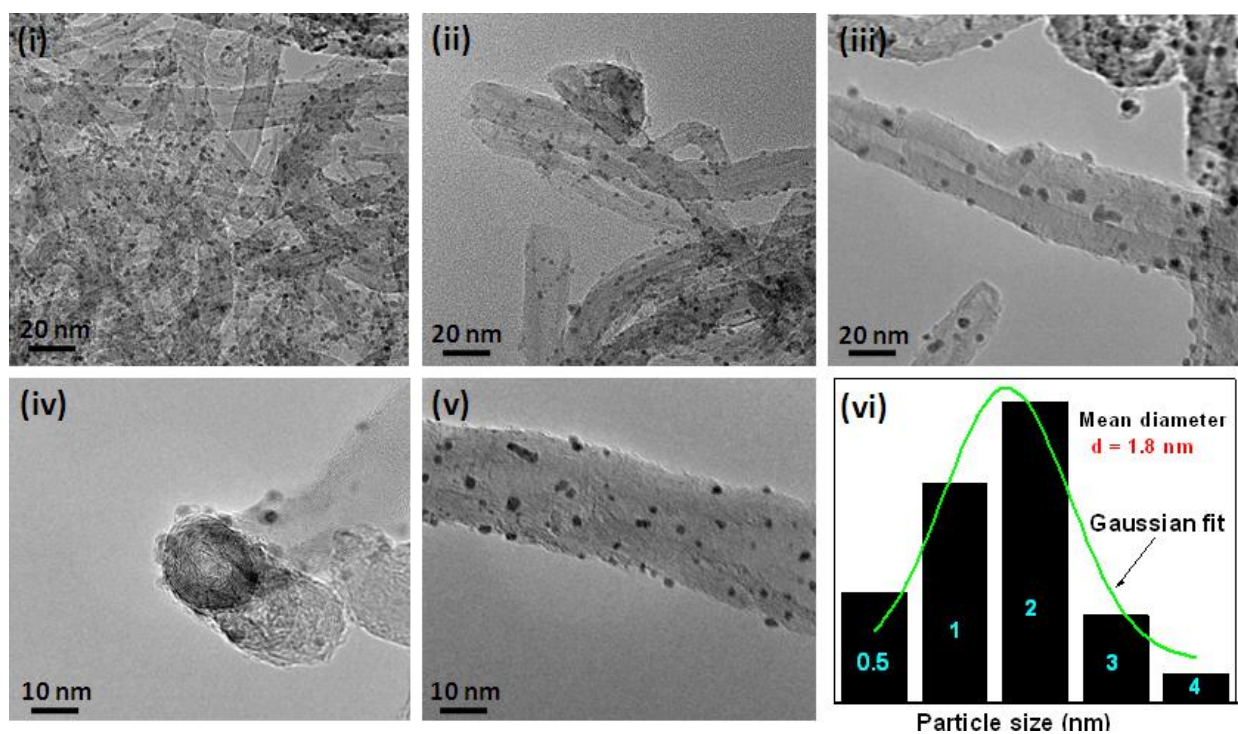
Fig. 2. (i, ii, iii, iv and v) TEM images of RuO_2/MWCNT and (vi) the particle size distribution of RuO_2NPs.
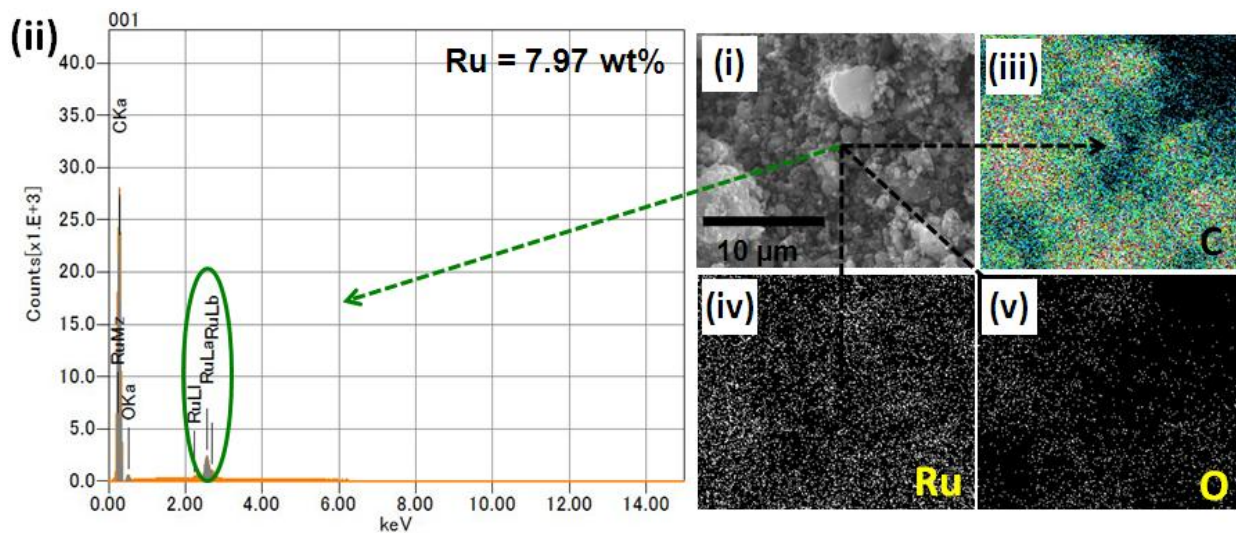
Fig. 3. (i) SEM image and (ii) EDS spectrum of RuO_2/MWCNT, and corresponding EDS mapping of (iii) C, (iv) Ru and (v) O.
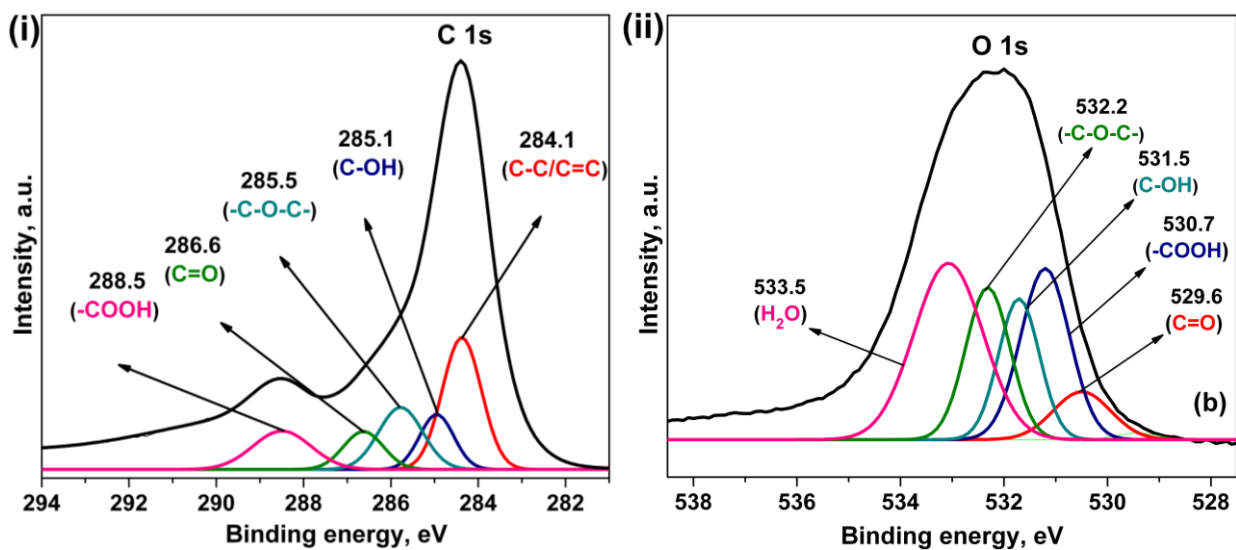
Fig. 4. XPS spectra of *f*-MWCNTs; magnified (i) C 1s and (ii) O 1s peaks.
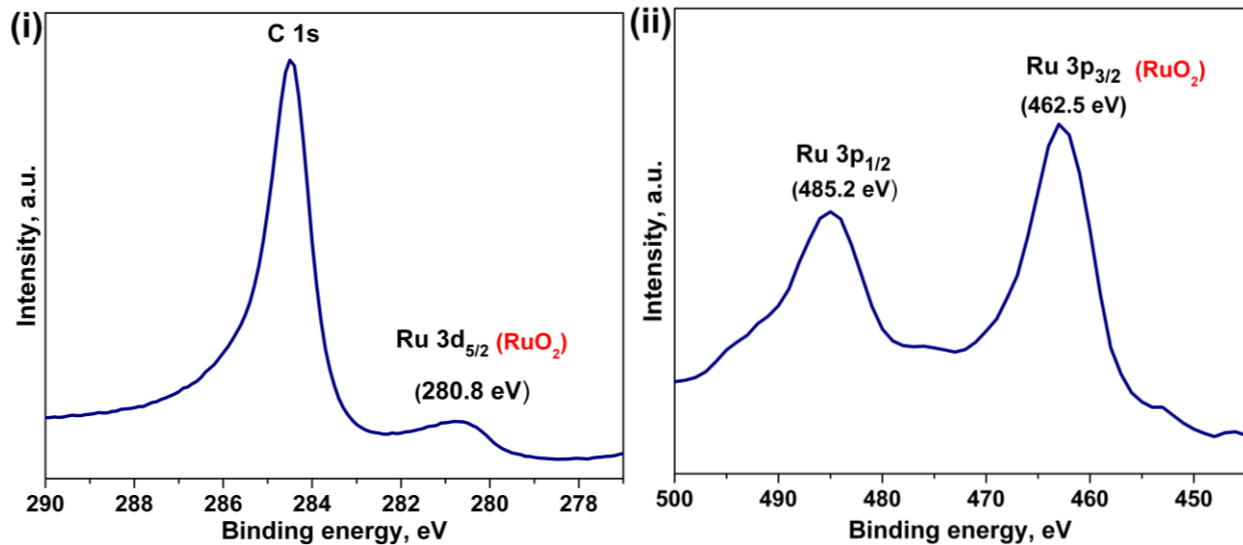
Fig. 5. XPS spectra of RuO$_2$/MWCNT; magnified (i) C 1s and (ii) Ru 3p peaks.
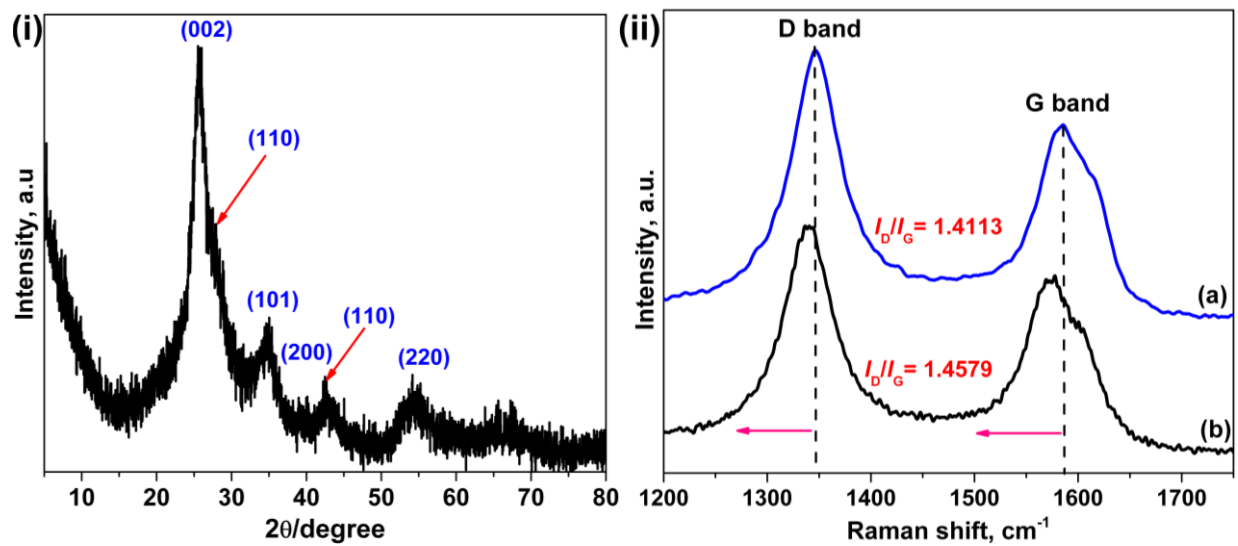
Fig. 6. (i) XRD pattern of RuO$_2$/MWCNT and (ii) Raman spectra of *f*-MWCNTs (**a**) and RuO$_2$/MWCNT (**b**).
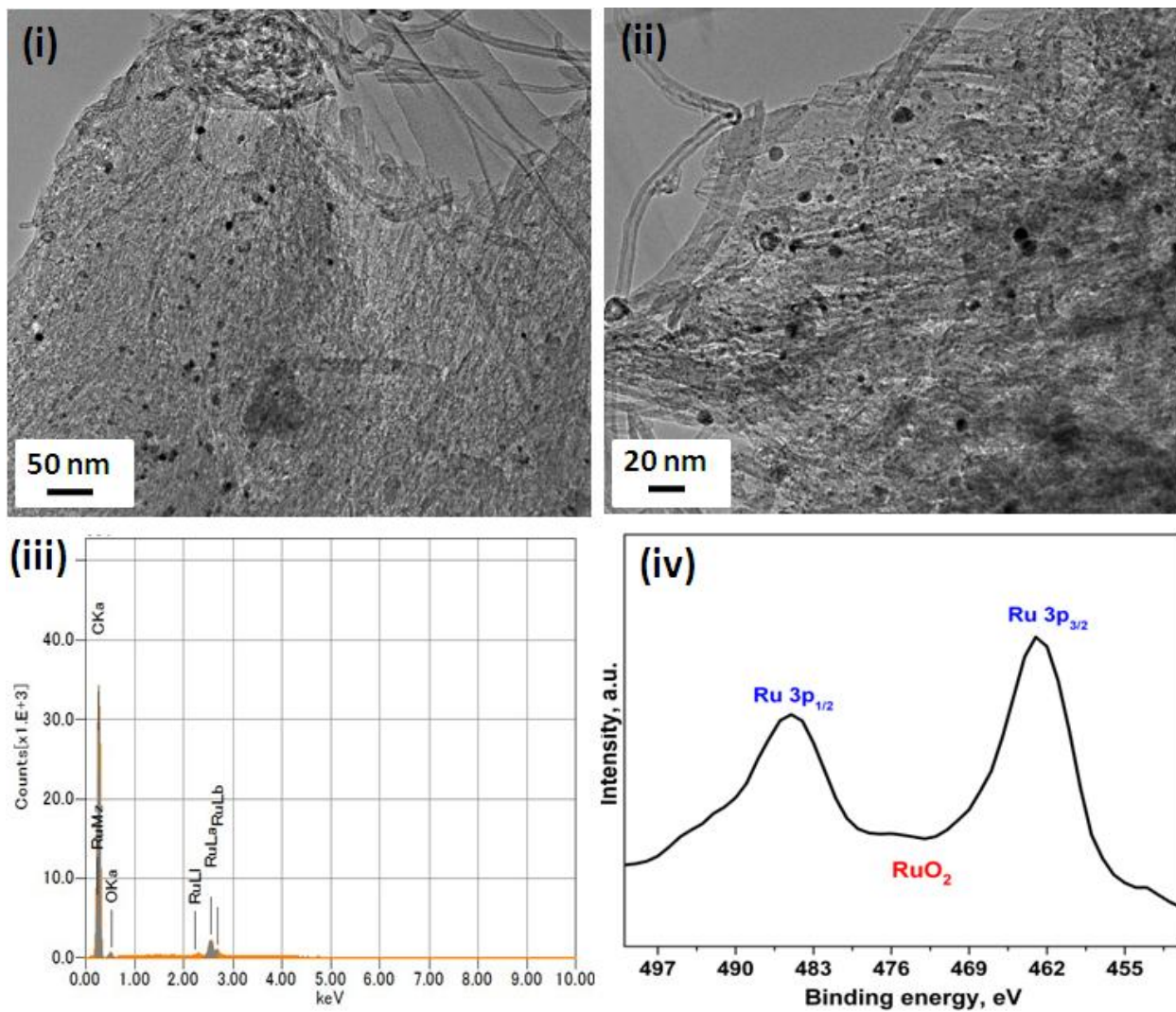
Fig. 7. (i and ii) TEM images of RuO$_2$/MWCNT, (iii) EDS spectrum of RuO$_2$/MWCNT and (iv) Ru 3p peaks of RuO$_2$/MWCNT.
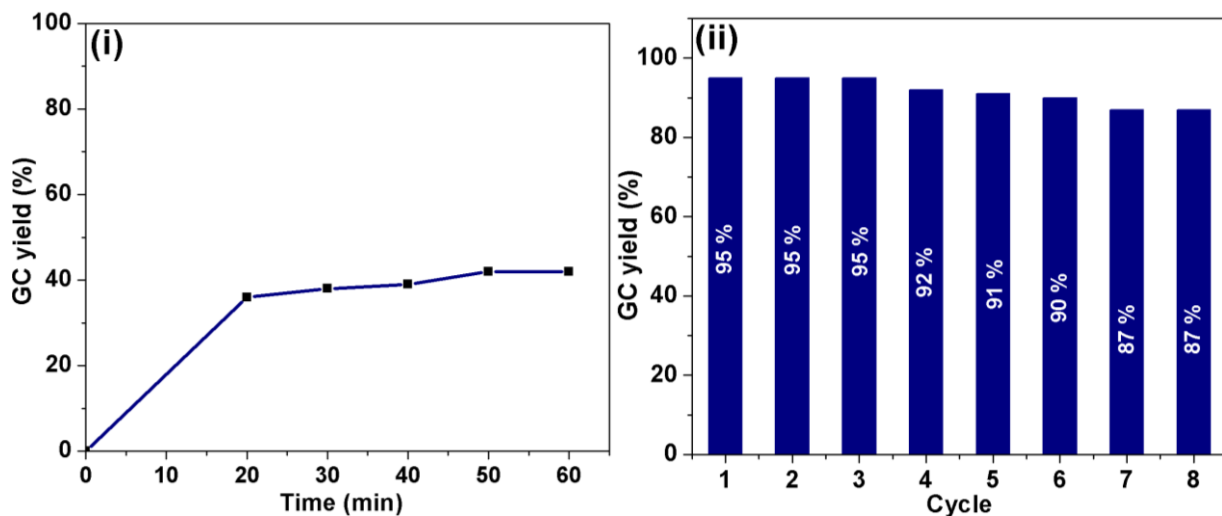
Fig. 8. (i) Heterogeneity and (ii) recyclability of RuO_2/MWCNT for transfer hydrogenation of acetophenone. [Reaction conditions: 117 µL of acetophenone (1 mmol), 80 mg of NaOH (1 mmol), 5 mg of RuO_2/MWCNT (0.77 mol %) and 5 mL of *i*-PrOH at 82°C for 45 min].
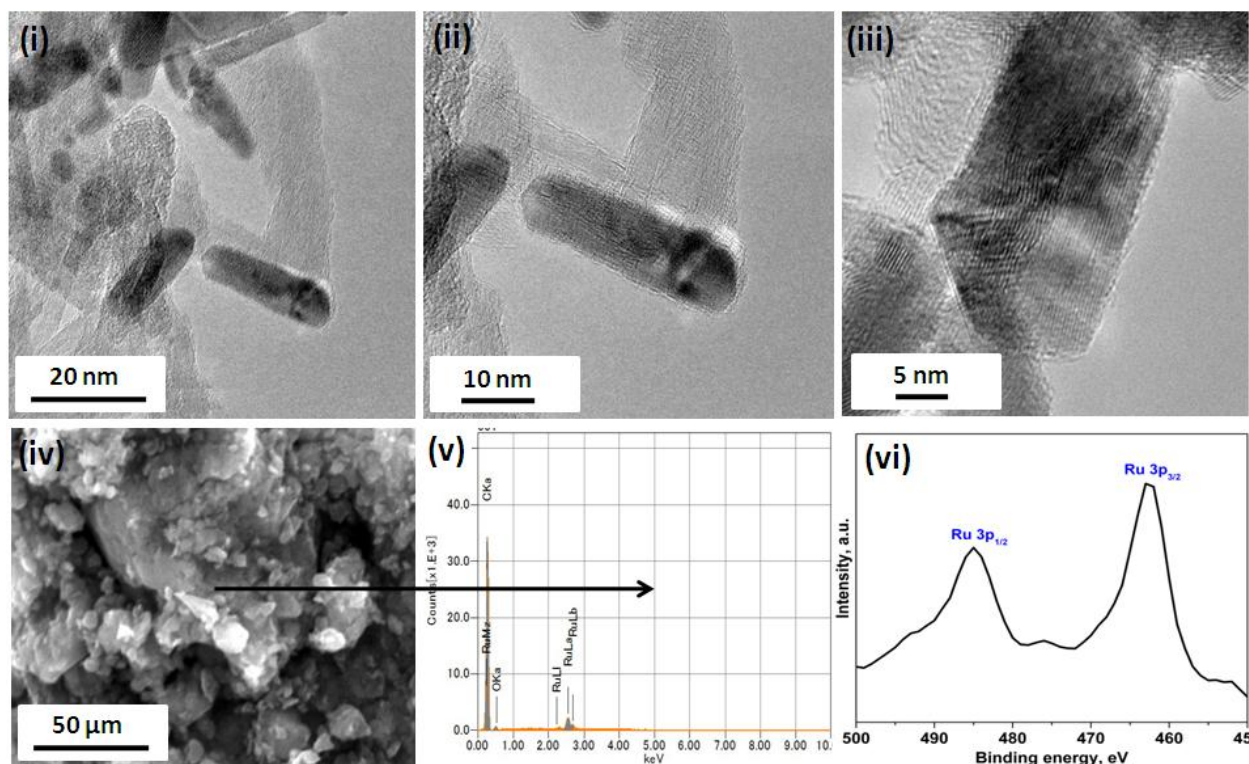
Fig. 9. (i, ii and iii) TEM images, (iv) SEM image, (v) EDS spctrum and (vi) Ru 3p peaks of *r*-RuO_2/MWCNT.

Supplementary Material
Click here to download Supplementary Material: Supplementary Material.R2.doc